Asian Journal of Probability and Statistics

Volume 26, Issue 9, Page 39-60, 2024; Article no.AJPAS.122072
ISSN: 2582-0230

Fractional Poisson and Gamma Models for Rainfall: Implications Climate Change and Marine Ecosystems

Khairia El-Said El-Nadi [a*], M. A. Abdou [b] and M. A. Fahmy [b]

[a] Department of Mathematics and Computer Science, Faculty of Science, Alexandria University, Egypt.
[b] Department of Mathematics, Faculty of Education, Alexandria University, Egypt.

Authors' contributions

This work was carried out in collaboration among all authors. All authors read and approved the final manuscript.

Article Information

DOI: https://doi.org/10.9734/ajpas/2024/v26i9645

Open Peer Review History:
This journal follows the Advanced Open Peer Review policy. Identity of the Reviewers, Editor(s) and additional Reviewers, peer review comments, different versions of the manuscript, comments of the editors, etc are available here: https://www.sdiarticle5.com/review-history/122072

Original Research Article

Received: 18/06/2024
Accepted: 20/08/2024
Published: 26/08/2024

Abstract

This research explores the benefits of using fractional Poisson and fractional Gamma models in rainfall modeling, highlighting their advantages in handling zero-inflated data, reducing overdispersion, and providing greater flexibility and accuracy.
The second part of this study delves into the dynamic interplay between oceanic ecosystems and global climate change. It focuses on the role of phytoplankton in oxygen production and the impact of warming waters on this delicate balance. By employing mathematical models integrating differential equations and Brownian motion, the study offers a comprehensive framework for understanding how varying rates of oxygen production influence the sustainability of oceanic ecosystems.
Finally, the research incorporates fractional Brownian motion into modeling plankton-oxygen dynamics, addressing the limitations of traditional Brownian motion. This approach captures the long-range

**Corresponding author: Email: Khairia_elsaid@hotmail.com, khairia_el_said@hotmail.com;*

Cite as: *El-Nadi, Khairia El-Said, M. A. Abdou, and M. A. Fahmy. 2024. "Fractional Poisson and Gamma Models for Rainfall: Implications Climate Change and Marine Ecosystems". Asian Journal of Probability and Statistics 26 (9):39-60. https://doi.org/10.9734/ajpas/2024/v26i9645.*

dependencies and persistent effects critical for predicting the response of marine ecosystems to climate change. The findings underscore the need for nuanced mitigation strategies to address the imminent risks posed by global warming on marine life and atmospheric oxygen levels.

Keywords: *Rainfall modeling; fractional Poisson process; fractional gamma distribution; plankton-oxygen dynamics; fractional Brownian motion.*

1 Introduction

Climate variables, especially the occurrence and intensity of rainfall, profoundly impact both natural and human environments. Understanding the frequency and intensity of rainfall events is vital for effectively planning, designing, and managing various water resource systems. This is particularly crucial for rain-fed agriculture, where crop production directly depends on the amount and timing of rainfall. Accurate rainfall modeling is essential not only for optimizing crop growth but also for developing weather derivatives, enhancing hydrological systems, and improving drought and flood management, as well as crop simulation studies (see [1]).

Rainfall modeling also plays a critical role in the financial sector, particularly in the pricing of weather derivatives. These financial instruments manage risks associated with adverse or unexpected weather conditions, providing a safeguard for various stakeholders, including farmers and investors. With the ongoing impacts of climate change, predicting rainfall variability for future periods under different climate change scenarios has become increasingly urgent (see [1]). Reliable predictions are essential for conducting high-quality climate impact studies, which in turn inform policy-making and adaptive strategies. These predictions help understand potential changes in rainfall patterns, enabling better preparation and response to the challenges posed by climate change.

However, modeling precipitation presents numerous challenges. These include accurately measuring precipitation, as rainfall data consists of sequences of zero or positive values (intensity) based on accumulation over discrete intervals. Additionally, factors like wind can affect measurement accuracy. Unlike temperature, which is highly correlated across regions, rainfall is localized; therefore, a derivative holder based on rainfall may face geographical basis risk when pricing weather derivatives. The final challenge is selecting an appropriate probability distribution function to describe precipitation data, as its statistical properties are complex and require a sophisticated distribution (see [2]).

Rainfall has frequently been modeled using chain-dependent processes, where the occurrence of rainfall on any given day depends on whether it rained on previous days. A commonly employed approach for this type of modeling is the two-state Markov chain model. In this model, there are two states: one representing the occurrence of rainfall (rainy state) and the other representing no rainfall (dry state). The transitions between these states are governed by certain probabilities that can be estimated from historical data. To model the intensity of rainfall how much it rains when it does rain statisticians fit a suitable probability distribution to the observed rainfall amounts. Commonly used distributions include the Gamma distribution (see [3]), the exponential distribution, and mixed exponential distributions. These distributions help describe the variability and frequency of different rainfall amounts (see [1] and see [4]).

One of the strengths of these models is their simplicity and interpretability. However, despite their advantages, these models have certain limitations. They require many parameters to accurately describe the complex dynamics of rainfall, which can make the models complicated and computationally intensive. Additionally, these models rely on several assumptions about the process, such as the independence of rainfall events from day to day and the appropriateness of the chosen distribution to fit the intensity of rainfall. If these assumptions do not hold true, the model's accuracy and reliability may be compromised.

This study aims to overcome these limitations by expanding upon previous research and utilizing fractional Poisson and fractional Gamma models to develop a fractional Poisson-Gamma model that previously given in [5]. This model aims to describe rainfall dynamics more accurately by considering the properties of zero-inflated data and reducing overdispersion. Specifically, the fractional Poisson process models the daily occurrence of rainfall, while the intensity is modeled using the fractional Gamma distribution as the magnitude of the jumps in the Poisson process. This results in a fractional compound Poisson process known as the fractional Poisson-Gamma model.

The fractional Poisson gamma model is particularly suitable for capturing the complexities associated with zero-inflated rainfall data and reducing overdispersion. By providing a more accurate representation of rainfall patterns, these models contribute to the development of more reliable climate prediction tools, which are essential for addressing the challenges imposed by climate change.

The second part of this study explores the dynamic interplay between oceanic ecosystems and global climate change. Oceans, covering nearly two-thirds of the Earth's surface, serve as a critical regulator of climate and atmospheric composition. Central to this regulation is phytoplankton, microscopic plants that perform photosynthesis, contributing approximately 70% of the Earth's atmospheric oxygen. However, this delicate balance is increasingly threatened by climate change, particularly global warming, which alters water temperatures and subsequently affects the rate of oxygen production by phytoplankton. The study employs mathematical models integrating differential equations to elucidate how varying rates of oxygen production influence the sustainability of these vital components (see [6]).

The final part of this research incorporates fractional Brownian motion into the modeling of plankton-oxygen dynamics under climate change. This approach offers a powerful tool for capturing the inherent randomness and complexity of natural systems. By integrating fractional Brownian motion, the study provides a more comprehensive and accurate understanding of the impact of climate change on plankton-oxygen dynamics. This approach contributes to the development of effective strategies for preserving marine ecosystems and maintaining atmospheric oxygen levels in the face of global warming.

This research underscores the significant implications of climate change on rainfall patterns, marine ecosystems, and atmospheric oxygen levels. It calls for a more nuanced understanding and proactive mitigation strategies to address the imminent risks posed by global warming. Through advanced modeling techniques, this study aims to provide valuable insights and tools for better predicting and managing the future impacts of climate change on our planet's vital systems.

The use of fractional Brownian motion to model the complexities of natural systems is particularly commendable.

This research offers a significant advancement in the field of climate change modeling by introducing fractional Poisson-Gamma models and fractional Brownian motion. These innovative approaches provide deeper insights into predicting rainfall patterns and understanding the complex dynamics of oxygen production in oceanic ecosystems. The findings of this study have the potential to improve climate models, which are crucial for developing strategies to mitigate the impacts of climate change. This insights provided by this study are invaluable for developing more accurate models that can guide effective environmental management and policy-making.

2 Model Description

2.1 Rainfall modeling using fractional Poisson-gamma distribution

Rainfall includes both discrete and continuous components. When there is no rainfall, the amount is discrete (essentially zero), whereas during rainfall, the amount is continuous. Traditional approaches often separate the modeling of occurrence and intensity of rainfall. Typically, the occurrence is modeled using a first-order or higher-order Markov chain process see [4]. Based on this occurrence model, various distributions such as Gamma, exponential, mixed exponential, and Weibull are used to model the amount of precipitation see [3]. These models rely on several assumptions and include multiple parameters to accurately capture the observed temporal dependence in the rainfall process.

However, rainfall data often exhibit overdispersion, attributed to factors such as clustering, unaccounted temporal correlation, or the inherent variability from Bernoulli trials with unequal event probabilities. Traditional stochastic models tend to underestimate this overdispersion, which can lead to an underestimation of the risks associated with low or high seasonal rainfall.

In this research, our goal is to find a unified model that simultaneously accounts for both the occurrence and intensity of rainfall. We propose using a fractional Poisson-Gamma probability distribution, which is capable of modeling both the exact zeros (no rainfall) and the positive amounts of rainfall together. Rainfall will be modeled as a fractional compound Poisson process with fractional Gamma-distributed jumps. This approach is motivated by the abrupt changes in rainfall amounts from zero to a significant positive value following each rainfall event, which are represented as jumps in the fractional compound Poisson process.

We assume that rainfall occurs in the form of storms, which follow a fractional Poisson process. At each arrival time, the current rainfall intensity increases by a random amount determined by a fractional Gamma distribution. The jumps in this process represent the arrival of storm events, each generating a random jump size. Each storm consists of cells that also arrive according to another fractional Poisson process.

2.2 Plankton-oxygen dynamics modeling under climate change

To explore the dynamics of plankton and oxygen under the influence of climate change, we incorporate a mathematical model based on a set of differential equations that describe the interactions between oxygen, phytoplankton, and zooplankton. The key components of the model are as follows see [6]:

1. **Oxygen Dynamics:** The concentration of oxygen (c) is influenced by its production through photosynthesis by phytoplankton (u) and its consumption through respiration by both phytoplankton and zooplankton (v). The rate of oxygen production is modeled as a function of the phytoplankton density and environmental factors such as water temperature.
2. **Phytoplankton Dynamics:** Phytoplankton density (u) changes due to growth, which is dependent on the available oxygen and light for photosynthesis. Phytoplankton also consume oxygen for respiration, and their growth is limited by intra-specific competition.
3. **Zooplankton Dynamics:** Zooplankton density (v) changes due to predation on phytoplankton and their own respiration, which consumes oxygen. The growth of zooplankton is influenced by the availability of phytoplankton as a food source.

In this study, incorporating Brownian motion into the modeling of plankton-oxygen dynamics under climate change provides a robust framework for capturing the inherent randomness and complexity of natural systems. Brownian motion is utilized to model the random fluctuations in environmental factors such as water temperature, which directly affect the rate of oxygen production by phytoplankton. This approach allows for the simulation of small-scale variability and randomness in nutrient availability and other environmental conditions, influencing phytoplankton growth and respiration.

2.3 Enhanced modeling with fractional Brownian motion

We describe the integration of fractional Brownian motion into our existing plankton-oxygen dynamics model. The equations presented leverage the unique properties of fractional Brownian motion to better represent the stochastic behavior of the system components. Fractional Brownian motion introduces long memory and self-similarity into the modeling framework, capturing the persistent dependencies and complex temporal correlations observed in ecological systems.

By incorporating fractional Brownian motion, we can more accurately simulate and understand the intricate dynamics of plankton and oxygen interactions in a changing climate. This enhanced modeling approach allows for better predictions of long-term impacts and provides deeper insights into the potential ecological consequences of global warming on marine ecosystems.

3 Mathematical Formulation

3.1 Rainfall modeling using fractional Poisson-gamma distribution

Let $N(t)$ be the total numbers of rainfall event per day, following a fractional Poisson process see [7] and see [8] such that:

$$P(N_t = n) = \int_0^\infty \xi_\alpha(\theta) e^{-\lambda^\alpha \theta} \frac{\lambda^{\alpha n} \theta^n}{n!} d\theta \tag{1}$$

Adapting equation (1) to become

$$\sum_{n=0}^{\infty} P(N_t = n) = \int_0^\infty \xi_\alpha(\theta) e^{-\lambda^\alpha \theta} \sum_{n=0}^{\infty} \frac{\lambda^{\alpha n} \theta^n}{n!} d\theta = 1 \ ,$$

Hence, we have

$$\int_0^\infty \xi_\alpha(\theta) d\theta = 1 \tag{2}$$

The total rainfall accumulation is calculated as the cumulative sum of individual rainfall events, denoted as $y_i, i \geq 1.$ Assuming each follows a symmetric and independently fractional Gamma distribution. Moreover, these distributions are assumed to be independent of the rainfall timing occurrences.

$$L(t) = \begin{cases} \sum_{i=0}^{N_r} y_i, & N_r = 1, 2, ..., n \\ 0 & N_r = 0 \end{cases} \tag{3}$$

Such that y_i ~ Fractional Gamma distributed with probability density function

$$f(y) = \int_0^\infty \xi_\alpha(\theta) \frac{\alpha^P \theta^P}{\Gamma(P)} y^{P-1} e^{-\alpha\theta y} d\theta \tag{4}$$

After integrating the previous formula with respect to y, $y \in [0, \infty)$, we have

$$\int_0^\infty f(y) dy = 1.$$

Lemma 1:

The compound fractional Poisson process (1) has a cumulant function given by

$$\ln M_L(s) = \ln\left(\sum_{j=0}^{\infty} \frac{((\lambda)^\alpha (M_Y(s) - 1))^j}{\Gamma(\alpha j + 1)}\right), \quad (0 \leq s < t). \tag{5}$$

where, $M_y(x), x \in \mathbb{R}$, is the moment generating function of the fractional gamma distribution.

Proof:

The moment generating function of $L(s)$ is given by:

$$M_L(s) = E(e^{sL(t)}) = \sum_{j=0}^{\infty} E(e^{sL(t)} \mid N(t) = j).P(N(t) = j)$$

$$= \sum_{j=0}^{\infty} E(e^{s(L(1)+L(2)+.....+L(j))} \mid N(t) = j)P(N(t) = j)$$

$$= \sum_{j=0}^{\infty} E(e^{s(L(1)+L(2)+.....+L(j))})P(N(t) = j))$$

$$= \sum_{j=0}^{\infty} (M_y(s))^j \int_0^{\infty} \xi_\alpha(\theta) e^{-\lambda^\alpha t^\alpha \theta} \frac{\lambda^{\alpha j} t^{\alpha j} \theta^j}{j!} d\theta$$

$$= \int_0^{\infty} \xi_\alpha(\theta) e^{-\lambda^\alpha t^\alpha \theta} \sum_{j=0}^{\infty} \frac{(M_y(s)\lambda^\alpha t^\alpha \theta)^j}{j!} d\theta$$

$$= \int_0^{\infty} \xi_\alpha(\theta) \exp(-\lambda^\alpha t^\alpha \theta + M_y(s)\lambda^\alpha t^\alpha \theta) d\theta$$

$$= \int_0^{\infty} \xi_\alpha(\theta) e^{\lambda^\alpha t^\alpha \theta (M_y(s)-1)} d\theta$$

$$= \sum_{j=0}^{\infty} \frac{((\lambda t)^\alpha (M_Y(s)-1))^j}{\Gamma(\alpha j+1)}$$

So, the cumulant function takes the form

$$\ln M_L(s) = \ln(\sum_{j=0}^{\infty} \frac{((\lambda t)^\alpha (M_Y(s)-1))^j}{\Gamma(\alpha j+1)}),$$

that can be adapted to take the final form

$$\ln M_L(s) = \ln(\sum_{} \frac{((\lambda t)^\alpha ((\Gamma(P)(\frac{\alpha}{s})^P)-1))^j}{}$$

When monitoring rainfall across n periods, then we have the sequence $\{L_i\}_{i=1}^n$ which are independent and identically distributed.

Result 1:

If there is no rainfall on a specific day, then we have:

$$P(L=0) = \int_0^{\infty} \xi_\alpha(\theta) e^{-\lambda^\alpha \theta} \frac{\lambda^{\alpha 0} \theta^0}{0!} d\theta = \sum_{i=0}^{\infty} \frac{(-\lambda^\alpha)^i}{\Gamma(\alpha i+1)} \tag{6}$$

Lemma 2:

The probability density function of L is:

$$(\sum_{i=0}^{\infty} \frac{(-\lambda^\alpha)^i}{\Gamma(\alpha i+1)})\delta_0(L) + \int_0^{\infty}\int_0^{\infty} \xi_\alpha(\theta_1)\xi_\alpha(\theta_2) L^{-1} e^{-\alpha\theta_1 L - \lambda^\alpha \theta_2} r_P(\upsilon L^P) d\theta_1 d\theta_2 \tag{7}$$

where $\delta_0(L)$ is the Dirac function at zero

Proof: Let $q_0 = 1 - p_0$, p_0 is given by (6), the probability that it rained. Hence for $L_i > 0$ we have

$$f_*^+(L) = \sum_{i=1}^{\infty} \frac{p_i}{q_0} \left(\int_0^{\infty} \xi_\alpha(\theta_1) \frac{\alpha^{iP} \theta_1^{iP} L^{iP-1} e^{-\alpha\theta_1 L}}{\Gamma(iP)} d\theta_1 \right)$$

The previous formula can take the form:

$$f_*^+(L) = \frac{1}{q_0} \left[\int_0^{\infty} \int_0^{\infty} \xi_\alpha(\theta_1) \xi_\alpha(\theta_2) e^{-\alpha\theta_1 L} e^{-\lambda^\alpha \theta_2} \left(\sum_{i=1}^{\infty} \frac{(\lambda^\alpha \theta_2)^i}{i!} \frac{(\alpha\theta_1)^{iP} L^{iP-1}}{\Gamma(iP)} \right) d\theta_1 d\theta_2 \right]$$

Using the value $q_0 = 1 - \sum_{i=0}^{\infty} \frac{(-\lambda^\alpha)^i}{\Gamma(\alpha i + 1)}$ to have:

$$f_*^+(L) = \int_0^{\infty} \int_0^{\infty} \xi_\alpha(\theta_1) \xi_\alpha(\theta_2) \frac{L^{-1} e^{-\alpha\theta_1 L} e^{-\lambda^\alpha \theta_2}}{1 - \sum_{i=0}^{\infty} \frac{(-\lambda^\alpha)^i}{\Gamma(\alpha i + 1)}} \left(\sum_{i=1}^{\infty} \frac{\lambda^\alpha \theta_2 \alpha^P \theta_1^P L^P}{i! \Gamma(iP)} \right) d\theta_1 d\theta_2$$

If we let $\upsilon = \lambda^\alpha \theta_2 \alpha^P$ and $r_P(\upsilon L^P) = \sum_{i=1}^{\infty} \frac{\upsilon \theta_1^P L^P}{i! \Gamma(iP)}$, we have

$$f_*^+(L) = \int_0^{\infty} \int_0^{\infty} \xi_\alpha(\theta_1) \xi_\alpha(\theta_2) \frac{L^{-1} e^{-\alpha\theta_1 L} e^{-\lambda^\alpha \theta_2}}{1 - \sum_{i=0}^{\infty} \frac{(-\lambda^\alpha)^i}{\Gamma(\alpha i + 1)}} r_P(\upsilon L^P) d\theta_1 d\theta_2 \tag{8}$$

We can express the probability density function $f_*(L)$ in terms of a Dirac function as

$$f_*(L) = p_0 \delta_0(L) + q_0 f_*^+(L)$$

Using the values of p_0, q_0, we have

$$f_*(L) = \left(\sum_{i=0}^{\infty} \frac{(-\lambda^\alpha)^i}{\Gamma(\alpha i + 1)} \right) \delta_0(L) + \int_0^{\infty} \int_0^{\infty} \xi_\alpha(\theta_1) \xi_\alpha(\theta_2) L^{-1} e^{-\alpha\theta_1 L - \lambda^\alpha \theta_2} r_P(\upsilon L^P) d\theta_1 d\theta_2. \tag{9}$$

The formula (9) represents a random sample of size n of L_i with the probability density function.

3.2 Plankton-oxygen dynamics modeling under climate change

Let (Ω, f, f_t, P) be a filtered probability space and let $\{W(t), t \geq 0\}$ be a standard Wiener process adapted to the filtration ($f_t, t \geq 0$), where $W_i(t)$, i =1,2,3 is independent see ([9] and see [10]).

Consider the following stochastic system see [6]:

Zooplankton Density (v) Equation:

$$dv(t) = \left[\frac{\eta c^2(t)}{c^2(t) + c_4^2} \frac{u(t)v(t)}{u(t) + h} - \mu v(t) \right] dt + \sigma_1 v(t) dW_1(t) \tag{10}$$

Here, η is the feeding efficiency of zooplankton, and μ represents the natural mortality rate of zooplankton. The Brownian term models the stochastic movement and distribution of zooplankton due to turbulent mixing.

Phytoplankton Density (u) Equation:

$$du(t) = [(\frac{Bc(t)}{c(t)+c_1} - u(t))u(t) - \frac{u(t)v(t)}{u(t)+h} - \sigma_2 u(t)]dt + \sigma_2 u(t)dW_2(t) \tag{11}$$

Here, B is the maximum per capita growth rate of phytoplankton, and σ_2 represents the natural mortality rate of phytoplankton. The Brownian term accounts for random environmental variations affecting phytoplankton growth.

Oxygen Concentration (c) Equation:

$$dc(t) = [\frac{Au(t)}{c(t)+1} - \frac{\delta u(t)c(t)}{c(t)+c_2} - \frac{v(t)c(t)v(t)}{c(t)+c_3} - c(t)]dt + \sigma_3 c(t)dW_3(t) \tag{12}$$

Here, A represents the rate of oxygen production, δ and ν are the respiration rates of phytoplankton and zooplankton, respectively, and mmm is the natural oxygen loss rate. The Brownian term represents the stochastic fluctuations due to environmental randomness.

The equations (10) – (12) can be reformulated as follows:

$$dv_1(t) = [\eta v_1(t) - \mu v_1(t)]dt + \sigma_1 v_1(t)dW_1(t) \text{ , Where } (v_1(t) \geq v(t)). \tag{13}$$

$$du_1(t) = [Bu_1(t) - \sigma_2 u_1(t)]dt + \sigma_2 u_1(t)dW_2(t) \text{ , Where } (u_1(t) \geq u(t)). \tag{14}$$

$$dc_1(t) = [Au_1(t) - c_1(t)]dt + \sigma_3 c_1(t)dW_3(t) \text{ , Where } (c_1(t) \geq c(t)). \tag{15}$$

Note: All parameters are nonnegative due to their biological significance.

Consider the following stochastic differential equations:

$$dX_i(t) = \frac{1}{2}\sigma_i^2 X_i(t)dt - \sigma_i X_i(t)dW_i(t), \tag{16}$$

$$dY_i(t) = \frac{1}{2}\sigma_i^2 Y_i(t)dt + \sigma_i Y_i(t)dW_i(t), (i = 1.2.3.) \tag{17}$$

Where, the solution of these two stochastic differential equations are given by (see [11]**):**

$$X_i(t) = e^{-\sigma_i W_i(t)} \tag{18}$$

$$Y_i(t) = e^{\sigma_i W_i(t)}, \quad (i = 1, 2, 3). \tag{19}$$

Now to solve equation (13): by using equation (16) (at i=1), we set $v_2(t) = X_1(t)v_1(t)$ and applying the formula of Ito, to get:

$$dv_2(t) = v_1(t)[\frac{1}{2}\sigma_1^2 X_1(t)dt - \sigma_1 X_1(t)dW_1(t)] + X_1(t)[[\eta v_1(t) - \mu v_1(t)]dt + \sigma_1 v_1(t)dW_1(t)] - \sigma_1^2 X_1(t)v_1(t)dt$$

$$dv_2(t) = \frac{1}{2}\sigma_1^2 v_2(t)dt - \sigma_1 v_2(t)dW_1(t) + \eta v_2(t)dt - \mu v_2(t)dt + \sigma_1 v_2(t)dW_1(t) - \sigma_1^2 v_2(t)dt$$

$$dv_2(t) = \frac{1}{2}\sigma_1^2 v_2(t)dt + \eta v_2(t)dt - \mu v_2(t)dt - \sigma_1^2 v_2(t)dt$$

$$dv_2(t) = v_2(t)[\eta - \mu - \frac{1}{2}\sigma_1^2]dt$$

$$\frac{dv_2(t)}{v_2(t)} = [\eta - \mu - \frac{1}{2}\sigma_1^2]dt$$

(After integrating, we have) $v_2(t) = e^{[\eta-\mu-\frac{1}{2}\sigma_1^2]t} v_1(0)$

$v_1(t) = e^{[\eta-\mu-\frac{1}{2}\sigma_1^2]t} X_1^{-1} v_1(0)$ (by taking expectation)

$$E(v_1(t)) = e^{[\eta-\mu-\frac{1}{2}\sigma_1^2]t} E(X_1^{-1}) v_1(0)$$

$$E(v_1(t)) = e^{(\eta-\mu)t} v_1(0) \quad (20)$$

Now: If $\eta < \mu$, then.

$$\lim_{t\to 0} E(v_1(t)) = 0$$

After taking the limit as t → 0, the physical meaning of the model's results emphasizes the immediate impact of initial conditions and the relationship between growth and mortality rates on the zooplankton population. The findings underscore the sensitivity of the system to initial disturbances and highlight the rapid response of the population dynamics to environmental variability. This understanding is crucial for predicting and managing the immediate effects of environmental changes on marine ecosystems.

To solve equation (14): by using equation (16) , (at i=2), we set $u_2(t) = X_2(t)u_1(t)$ and applying the formula of Ito, to get:

$$du_2(t) = u_1(t)[\frac{1}{2}\sigma_2^2 X_2(t)dt - \sigma_2 X_2(t)dW_2(t)] + X_2(t)[[Bu_1(t) - \sigma_2 u_1(t)]dt + \sigma_2 u_1(t)dW_2(t)] - \sigma_2^2 X_2(t)u_1(t)dt$$

$$du_2(t) = \frac{1}{2}\sigma_2^2 u_2(t)dt - \sigma_2 u_2(t)dW_2(t) + Bu_2(t)dt - \sigma_2 u_2(t)dt + \sigma_2 u_2(t)dW_2(t) - \sigma_2^2 u_2(t)dt$$

$$du_2(t) = Bu_2(t)dt - \sigma_2 u_2(t)dt - \frac{1}{2}\sigma_2^2 u_2(t)dt$$

$$du_2(t) = u_2(t)[B - \sigma_2 - \frac{1}{2}\sigma_2^2]dt$$

$$\frac{du_2(t)}{u_2(t)} = [B - \sigma_2 - \frac{1}{2}\sigma_2^2]dt \quad \text{(After integrating, we have)}$$

$$u_2(t) = e^{[B-\sigma_2-\frac{1}{2}\sigma_2^2]t} u_1(0)$$

$u_1(t) = e^{[B-\sigma_2-\frac{1}{2}\sigma_2^2]t} X_2^{-1} u_1(0)$ (by taking expectation) (21)

$$E(u_1(t)) = e^{[B-\sigma_2-\frac{1}{2}\sigma_2^2]t} E(X_2^{-1}) u_1(0)$$

$$E(u_1(t)) = e^{[B-\sigma_2]t} u_1(0) \quad (22)$$

Now: If $B < \sigma_2$, then

$$\lim_{t\to 0} E(u_1(t)) = 0$$

After taking the limit as t → 0, the physical meaning of the model's results indicates that when the intrinsic growth rate of phytoplankton is lower than the intensity of environmental fluctuations, the phytoplankton population is expected to decline to zero initially. This highlights the critical impact of environmental disturbances on phytoplankton sustainability and the broader implications for marine ecosystem health and stability.

The solution of equation (15) by using equation (21) given by:

$$c_1(t) = c_1(0) + \int_0^t Ae^{[B-\sigma_2-\frac{1}{2}\sigma_2^2]s} e^{\sigma_2 W_2(s)} u_1(0)ds - \int_0^t c_1(s)ds + \sigma_3 \int_0^t c_1(s)dW_3(s)$$

By taking expectation: -

$$E(c_1(t)) = c_1(0) + \int_0^t Ae^{[B-\sigma_2-\frac{1}{2}\sigma_2^2]s} E(e^{\sigma_2 W_2(s)})u_1(0)ds - \int_0^t E(c_1(s))ds + \sigma_3 E(\int_0^t c_1(s)dW_3(s))$$

The above equation is adapted in the form:

$$E(c_1(t)) = c_1(0) + \int_0^t Ae^{[B-\sigma_2]s} u_1(0)ds - \int_0^t E(c_1(s))ds$$

Rearrange the equation:

$$E(c_1(t)) + \int_0^t E(c_1(s))ds = c_1(0) + \int_0^t Ae^{[B-\sigma_2]s} u_1(0)ds$$

Differentiate the equation with respect to t:

$$\frac{d}{dt}E(c_1(t)) + E(c_1(t)) = \frac{d}{dt}[c_1(0) + \int_0^t Ae^{[B-\sigma_2]s} u_1(0)ds]$$

Now, we have a first order linear differential equation, we will apply the integrating factor:

$$\frac{d}{dt}[e^t E(c_1(t))] = Ae^{[B-\sigma_2]t} e^t u_1(0)$$

$$\frac{d}{dt}[e^t E(c_1(t))] = Ae^{[B-\sigma_2+1]t} u_1(0)$$

By integrate with respect to t:

$$e^t E(c_1(t)) - E(c_1(0)) = Au_1(0)\frac{e^{[B-\sigma_2+1]t} - 1}{(B-\sigma_2+1)}$$

Finally, we have

$$E(c_1(t)) = e^{-t}E(c_1(0)) + Ae^{t}u_1(0)\frac{1}{(1-B+\sigma_2)}[1-e^{-[1-B+\sigma_2]t}] \tag{23}$$

By taking limit $\lim_{t\to\infty} c^*(t) = \infty$

After taking the limit as t → ∞, the physical meaning of the model's results indicates that the modeled oxygen concentration increases indefinitely over time, suggesting continuous and unbounded oxygen production. These highlights potential oversimplifications in the model and underscores the importance of incorporating realistic feedback mechanisms and limiting factors to ensure a more accurate representation of ecological dynamics. Understanding these dynamics is crucial for predicting the long-term stability and sustainability of marine ecosystems.

3.3 Enhanced Modeling with Fractional Brownian Motion

Let $W_\alpha(t)$ be the fractional Brownian motion defined in [12], [13] and [14].

Consider the previous stochastic system equations (13) to (15). To solve it in view of fractional Brownian motion, we consider the following stochastic differential equations:

Zooplankton Density (v**) Equation:**

By using equation (13) but in fractional form:

$$dv_1(t) = [\eta v_1(t) - \mu v_1(t)]dt + \sigma_1 v_1(t)dW_{1,\alpha}(t) \text{ , Where } (v_1(t) \geq v(t)). \tag{24}$$

We consider the stochastic differential equations:

$$dX_i(t) = \frac{1}{2}\frac{t^{\alpha-1}}{\Gamma(\alpha)}\sigma_i{}^2 X_i(t)dt - \sigma_i X_i(t)dW_{i,\alpha}(t) \tag{25}$$

$$dY_i(t) = \frac{1}{2}\frac{t^{\alpha-1}}{\Gamma(\alpha)}\sigma_i{}^2 Y_i(t)dt + \sigma_i Y_i(t)dW_{i,\alpha}(t) \tag{26}$$

Where i=1,2,3, 0 < α < 1, $\Gamma(.)$ is Gamma function.

The solution of these two stochastic differential equations are given by:

$$X_i(t) = e^{-\sigma_i W_{i,\alpha}(t)} \tag{27}$$

$$Y_i(t) = e^{\sigma_i W_{i,\alpha}(t)} \tag{28}$$

Where i =1,2,3.

Now to solve equation (24): by using equation (25) (at i=1), we set $v_2(t) = X_1(t)v_1(t)$ and applying the formula of Ito, to get:

$$dv_2(t) = v_1(t)[\frac{1}{2}\frac{t^{\alpha-1}}{\Gamma(\alpha)}\sigma_1{}^2 X_1(t)dt - \sigma_1 X_1(t)dW_{1,\alpha}(t)] + X_1(t)[[\eta v_1(t) - \mu v_1(t)]dt + \sigma_1 v_1(t)dW_{1,\alpha}(t)] - \sigma^2{}_1 X_1(t)v_1(t)dt$$

$$dv_2(t) = \frac{1}{2}\sigma_1^2 \frac{t^{\alpha-1}}{\Gamma(\alpha)} v_2(t)dt - \sigma_1 v_2(t)dW_{1,\alpha}(t) + \eta v_2(t)dt - \mu v_2(t)dt + \sigma_1 v_2(t)dW_{1,\alpha}(t) - \sigma_1^2 v_2(t)dt$$

$$dv_2(t) = \eta v_2(t)dt - \mu v_2(t)dt + \frac{1}{2}\sigma_1^2 \frac{t^{\alpha-1}}{\Gamma(\alpha)} v_2(t)dt - \sigma_1^2 v_2(t)dt$$

$$dv_2(t) = v_2(t)[\eta - \mu + \frac{1}{2}\sigma_1^2 \frac{t^{\alpha-1}}{\Gamma(\alpha)} - \sigma_1^2]dt$$

$$\frac{dv_2(t)}{v_2(t)} = [\eta - \mu + \frac{1}{2}\sigma_1^2 \frac{t^{\alpha-1}}{\Gamma(\alpha)} - \sigma_1^2]dt \qquad \text{(After integrating, we have)}$$

$$v_2(t) = e^{[\eta-\mu-\sigma_1^2]t+\frac{1}{2}\sigma_1^2\frac{t^\alpha}{\Gamma(\alpha+1)}} v_1(0)$$

$$v_1(t) = e^{[\eta-\mu-\sigma_1^2]t+\frac{1}{2}\sigma_1^2\frac{t^\alpha}{\Gamma(\alpha+1)}} X_1^{-1} v_1(0) \qquad \text{(by taking expectation)}$$

$$E(v_1(t)) = e^{[\eta-\mu-\sigma_1^2]t+\frac{1}{2}\sigma_1^2\frac{t^\alpha}{\Gamma(\alpha+1)}} E(X_1^{-1}) v_1(0)$$

$$E(v_1(t)) = e^{[\eta-\mu-\sigma_1^2]t+\frac{1}{2}\sigma_1^2\frac{t^\alpha}{\Gamma(\alpha+1)}} \sum_{k=0}^{\infty} \frac{(\sigma_1^2 t^\alpha)^k}{2^k \Gamma(\alpha k+1)} . E(v_1(0)) \qquad (29)$$

Phytoplankton Density (u) Fractional Equation:

By using equation (14) but in fractional form:

$$du_1(t) = [Bu_1(t) - \sigma_2 u_1(t)]dt + \sigma_2 u_1(t)dW_{2,\alpha}(t) \text{ , Where } (u_1(t) \geq u(t)). \qquad (30)$$

Now to solve equation (30): by using equation (25) (at i=2), we set $u_2(t) = X_2(t)u_1(t)$ and applying the formula of Ito, to get:

$$du_2(t) = u_1(t)[\frac{1}{2}\frac{t^{\alpha-1}}{\Gamma(\alpha)}\sigma_2{}^2 X_2(t)dt - \sigma_2 X_2(t)dW_{2,\alpha}(t)] + X_2(t)[[Bu_1(t) - \sigma_2 u_1(t)]dt + \sigma_2 u_1(t)dW_{2,\alpha}(t)] - \sigma_2^2 X_2(t)u_1(t)dt$$

$$du_2(t) = \frac{1}{2}\frac{t^{\alpha-1}}{\Gamma(\alpha)}\sigma_2^2 u_2(t)dt - \sigma_2 u_2(t)dW_{2,\alpha}(t) + Bu_2(t)dt - \sigma_2 u_2(t)dt + \sigma_2 u_2(t)dW_{2,\alpha}(t) - \sigma_2^2 u_2(t)dt$$

$$du_2(t) = \frac{1}{2}\frac{t^{\alpha-1}}{\Gamma(\alpha)}\sigma_2^2 u_2(t)dt + Bu_2(t)dt - \sigma_2 u_2(t)dt - \sigma_2^2 u_2(t)dt$$

$$du_2(t) = u_2(t)[\frac{1}{2}\sigma_2^2 \frac{t^{\alpha-1}}{\Gamma(\alpha)} + B - \sigma_2 - \sigma_2^2]dt$$

$$\frac{du_2(t)}{u_2(t)} = [\frac{1}{2}\sigma_2^2 \frac{t^{\alpha-1}}{\Gamma(\alpha)} + B - \sigma_2 - \sigma_2^2]dt \qquad \text{(After integrating, we have)}$$

$$u_2(t) = e^{[B-\sigma_2+\sigma_2^2)t+\frac{1}{2}\sigma_2^2\frac{t^\alpha}{\Gamma(\alpha+1)}} u_1(0)$$

$$u_1(t) = e^{[B-\sigma_2+\sigma_2^2)t+\frac{1}{2}\sigma_2^2\frac{t^\alpha}{\Gamma(\alpha+1)}} u_1(0) X_2^{-1}$$

$$u_1(t) = e^{[B-\sigma_2+\sigma_2^2)t+\frac{1}{2}\sigma_2^2\frac{t^\alpha}{\Gamma(\alpha+1)}}u_1(0)e^{\sigma_2 w_{2,\alpha}(t)} \quad \text{(by taking expectation)}$$

$$E(u_1(t) = e^{[B-\sigma_2+\sigma_2^2)t+\frac{1}{2}\sigma_2^2\frac{t^\alpha}{\Gamma(\alpha+1)}}\sum_{k=0}^{\infty}\frac{(\sigma_2 t^\alpha)^k}{2^K\Gamma(1+\alpha k)}E(u_1(0)) \tag{31}$$

Oxygen Concentration (c) Fractional Equation:

By using equation (15) but in fractional form:

$$dc_1(t) = [Au_1(t) - c_1(t)]dt + \sigma_3 c_1(t)dW_{3,\alpha}(t) \text{ , Where } (c_1(t) \geq c(t)). \tag{32}$$

Where:

$$c_1(t) = c_1(0) + \int_0^t Au_1(s)ds - \int_0^t c_1(s)ds + \sigma_3\int_0^t c_1(s)dW_{3,\alpha}(s) \quad \text{(by taking expectation)}$$

$$E(c_1(t)) = c_1(0) + \int_0^t AE(u_1(s))ds - \int_0^t E(c_1(s))ds \tag{33}$$

Where E($W_{3,\alpha}(s)$)=0.

Assume

$$\gamma(t) = c_1(0) + \int_0^t AE(u_1(s))ds \text{ , } \quad E(c_1(t)) = F(t)$$

So, we get:

$$F(t) = \gamma(t) - \int_0^t F(s)ds \quad \text{(By taking derivative)}$$

$$\frac{d}{dt}F(t) = \frac{d}{dt}[\gamma(t) - \int_0^t F(s)ds]$$

$$\frac{d}{dt}F(t) = \gamma'(t) - F(t)$$

$$\frac{d}{dt}F(t) + F(t) = \gamma'(t) \quad \text{(solving the first order linear differential equation)}$$

The integrator factor is e^t , multiply the I.F. in the equation

$$\frac{d}{dt}(e^t F(t)) + e^t F(t) = e^t\gamma'(t)$$

$$e^t F(t) = \int_0^t e^s\gamma(s)ds$$

So, we get:

$$F(t) = e^{-t}\int_0^t e^s\gamma(s)ds \tag{34}$$

4 Data Analysis

4.1 Analysis of fractional Poisson gamma model

Analysis of the effect of α on fractional Poisson process

In this analysis, we will compare two different definitions of the function $\zeta_\alpha(\theta)$ used in the fractional Poisson process equation (1):

First Definition of $\zeta_\alpha(\theta)$ is given by:

$$\zeta_\alpha(\theta) = \frac{\theta^{\alpha-1}}{\Gamma(\alpha)}$$

Where $0 < \alpha < 1$ and $\Gamma(\alpha)$ is gamma function.

Second Definition of $\zeta_\alpha(\theta)$ is given by:

$$\zeta_\alpha(\theta) = \frac{\alpha\theta^{\alpha-1}}{t^\alpha} E_\alpha\left(\frac{-\theta^\alpha}{t^\alpha}\right)$$

Where this definition involves the Mittag-Leffler function.

Now, by using the first definition of $\zeta_\alpha(\theta)$, Fig. (1) shows the probability distribution changes subtly with variations in the value of λ at time t=0.001.

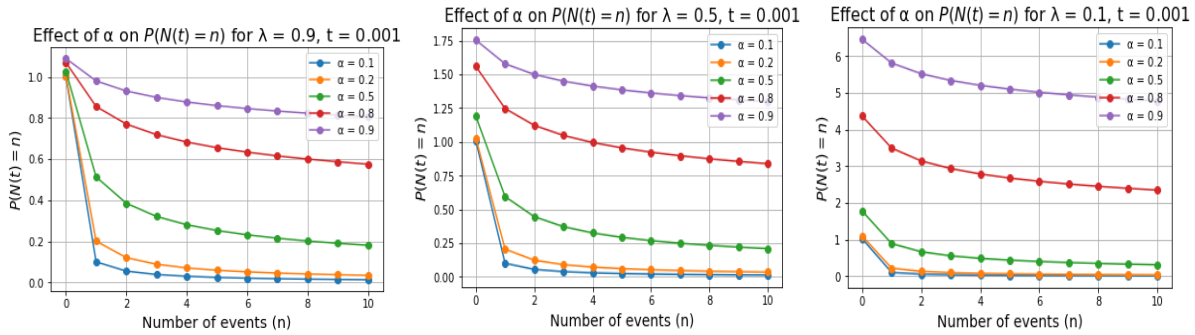

Fig. 1. The effect of α on fractional Poisson process for different values of λ using first zeta

As the number of events n increases, the probabilities tend to stabilize at low values. This indicates that the fractional Poisson distribution tends to converge towards a stable distribution as the number of events increases.

With increasing α values, the probabilities for fewer events are higher, reflecting a wider and more dispersed distribution, although the probabilities for fewer events are higher with larger α values, as n increases, the probabilities tend to stabilize at low values.

The effect of λ is noticeable, as increasing λ leads to higher concentration of probabilities for fewer events, despite this concentration, with increasing n, the distribution stabilizes at low values, indicating a combined effect of λ and α in shaping the probability distribution.

Overall, the graph shows that the fractional Poisson distribution tends to stabilize with increasing n, where probabilities for larger events decrease significantly and stabilize at low values. Both λ and α are important factors influencing the probability distribution, and the graphs illustrate how the dynamics can change based on these parameter values.

Now, by using the second definition of $\zeta_\alpha(\theta)$, Fig. (2) shows the probability distribution changes subtly with variations in the value of λ at time t=0.001.

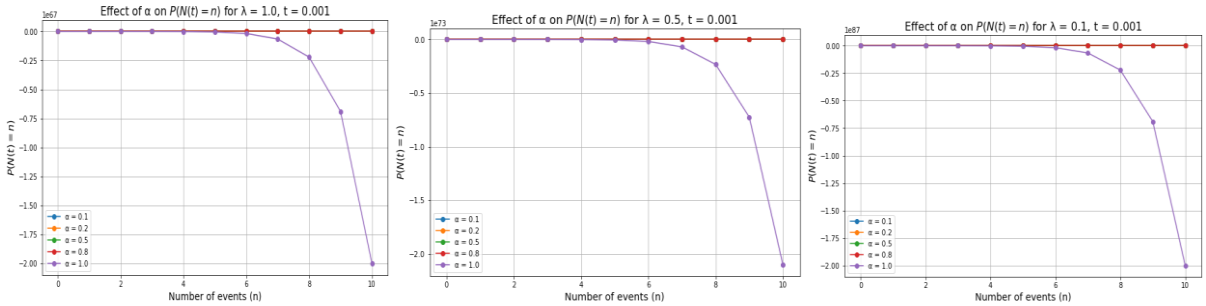

Fig. 2. The effect of α on fractional Poisson process for different values of λ using second zeta.

Stabilization with Increasing n: All graphs show that the distribution stabilizes at low values with increasing n, indicating that the fractional Poisson distribution converges towards a stable distribution as the number of events increases.

Effect of α: In all graphs, higher α values lead to higher probabilities for fewer events, reflecting a wider and more dispersed distribution. As n increases, the probabilities stabilize at low values.

Effect of λ: Increasing λ leads to a more concentrated distribution for fewer events. The probabilities for larger events decrease significantly and stabilize at low values, indicating a combined effect of λ and α in shaping the probability distribution.

By comparing the two definitions of $\zeta_\alpha(\theta)$, we can observe that both approaches exhibit similar trends in the fractional Poisson process.

Analysis of the cumulant function: Fig. (3) demonstrates the behavior of the cumulant function given in equation (4), where $0 < \alpha < 1$, P = 0.5, λ = 0.5 and s in range from 0.1 to 5.

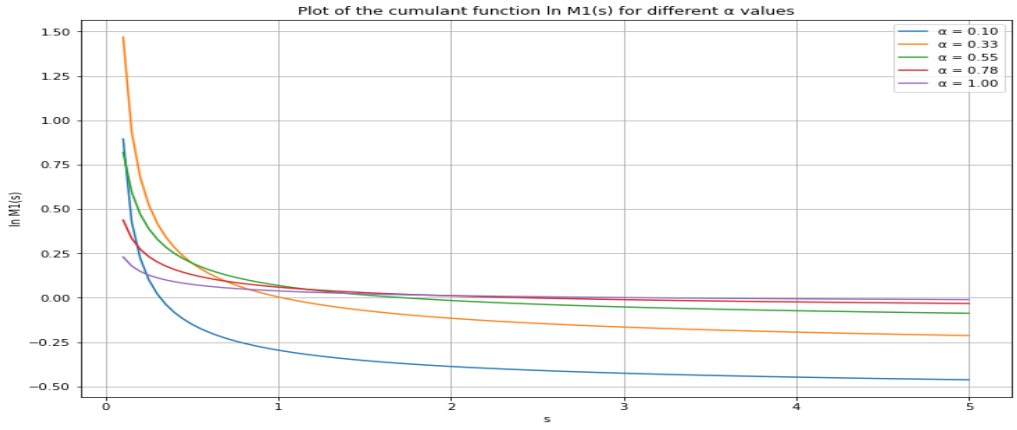

Fig. 3. The effect of α on the cumulant function

The cumulant function $\ln M_L(s)$ exhibits a strong dependence on the parameter α. For smaller α values, the function is initially higher and decreases more rapidly, indicating a higher sensitivity to s. As α increases, the initial value of the function decreases, and the curve becomes flatter, showing less sensitivity to changes in s. This behavior highlights the importance of the parameter α in controlling the shape and characteristics of the cumulant function $\ln M_L(s)$.

Analysis of the rainfall timing occurrences

Fig. (4) shows the effect of different α values on equation (8) over the range of L values from 0.1 to 2, with λ=0.5, p=0.5 and $\zeta_\alpha(\theta) = \dfrac{\theta^{\alpha-1}}{\Gamma(\alpha)}$.

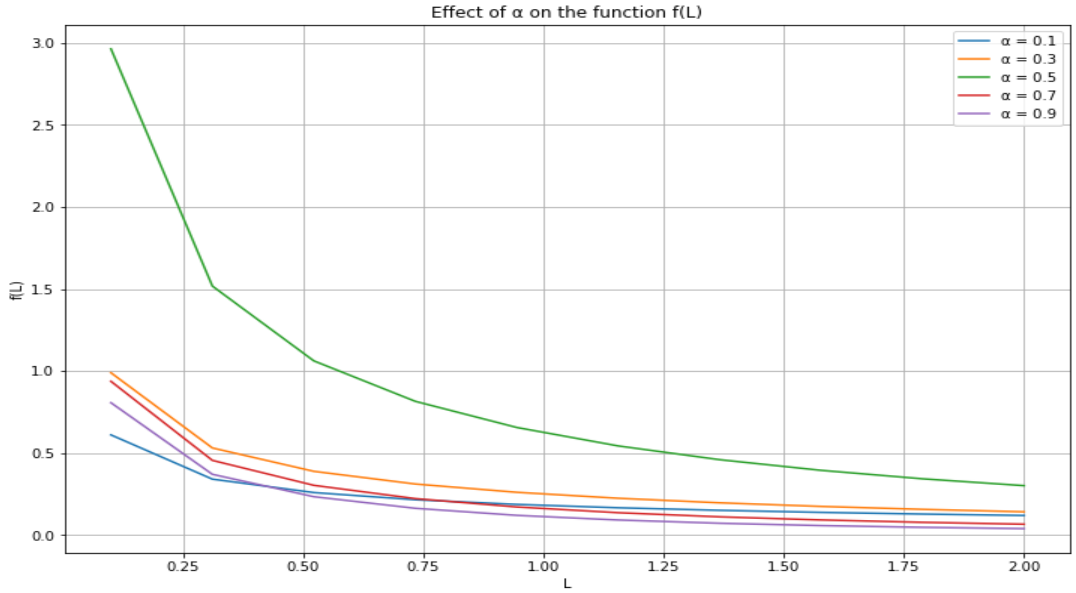

Fig. 4. The effect of alpha on rainfall occurrence

The analysis shows that α significantly influences the behavior of the function $f_*^+(L)$. Higher α values result in a more stable and positive $f_*^+(L)$, while lower α values cause $f_*^+(L)$ to decrease more rapidly. Understanding this relationship is crucial for applications that rely on tuning the parameter α to achieve desired outcomes.

4.2 Analysis of plankton-oxygen dynamics modeling under climate change

Analysis for zooplankton: To examine the scenario where the feeding efficiency (η) of zooplankton is less than their natural mortality rate (μ), we will base our analysis on scientific parameters derived from where the maximum feeding efficiency η for zooplankton is typically less than 1.0. Specifically, we will consider the following values: feeding efficiency (η = 0.2). and the natural mortality rate for zooplankton is (μ = 0.3).

If η < μ, this means the natural mortality rate of zooplankton is greater than their feeding efficiency. In this scenario, the population of zooplankton is expected to decline over time. The exponential term (η − μ) becomes negative, leading to an exponential decay of the population. Therefore, equation (20) describes a decreasing exponential function. As t increases, $e^{(\eta-\mu)t}$ approaches zero, causing the zooplankton population $v_1(t)$ to decrease toward zero. Fig. (5) shows zooplankton decay over time.

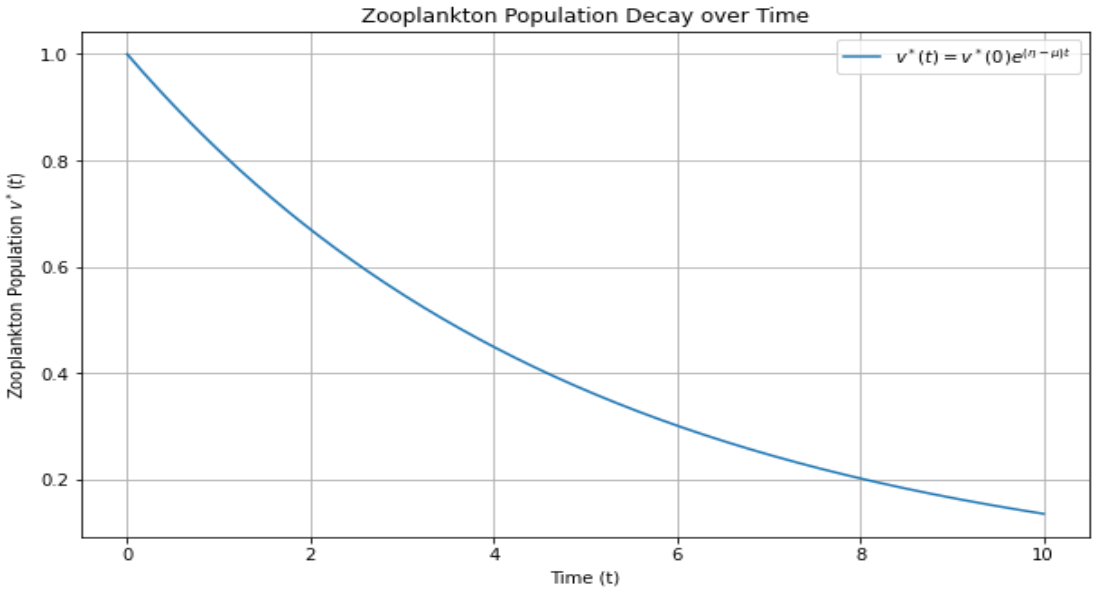

Fig. 5. Zooplankton decay over time

Fig. (5) shows the simulated zooplankton population over time when the natural mortality rate is greater than the feeding efficiency. The population starts from an initial value of $v_1(0) = 1.0$ and declines exponentially over time due to the negative difference between feeding efficiency and mortality rate.

Analysis for phytoplankton: When B < σ2, the system modeled by the equation (22) will exhibit exponential decay. This scenario is important for understanding how systems respond to high variability or noise, where the maximum per capita growth rate of phytoplankton B = 0.1, and the natural mortality rate of phytoplankton σ2=0.5.

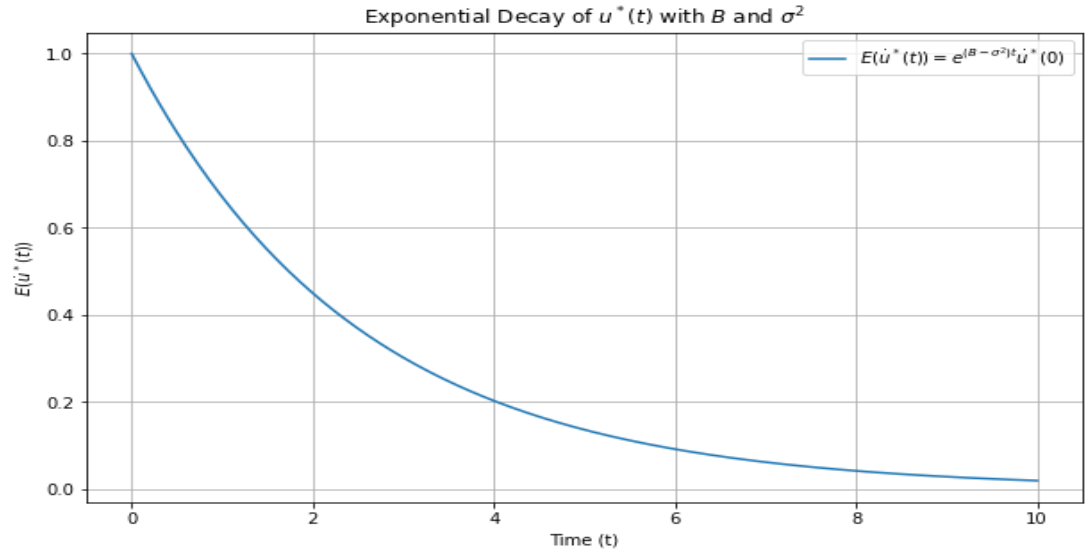

Fig. 6. Phytoplankton decay over time

Fig. (6) shows When B < σ2, the phytoplankton population modeled by equation (22) exhibits exponential decay. This scenario highlights the impact of high environmental variability or stress, leading to a damping effect that reduces the population over time. Such insights are critical for managing and predicting the behavior of phytoplankton populations in the face of significant environmental fluctuations.

Analysis for Oxygen Dynamics: The equation (23) modeling the expected value $E(c_1(t))$ illustrates how the concentration of oxygen changes over time, influenced by the initial concentration and other parameters.

Fig. (7) shows that the expected value $E(c_1(t))$ models the change in oxygen concentration over time, influenced by the initial concentration and parameters such as, the rate of oxygen production (A = 2.05), The maximum per capita growth rate of phytoplankton (B = 1.8), (σ =0.1).

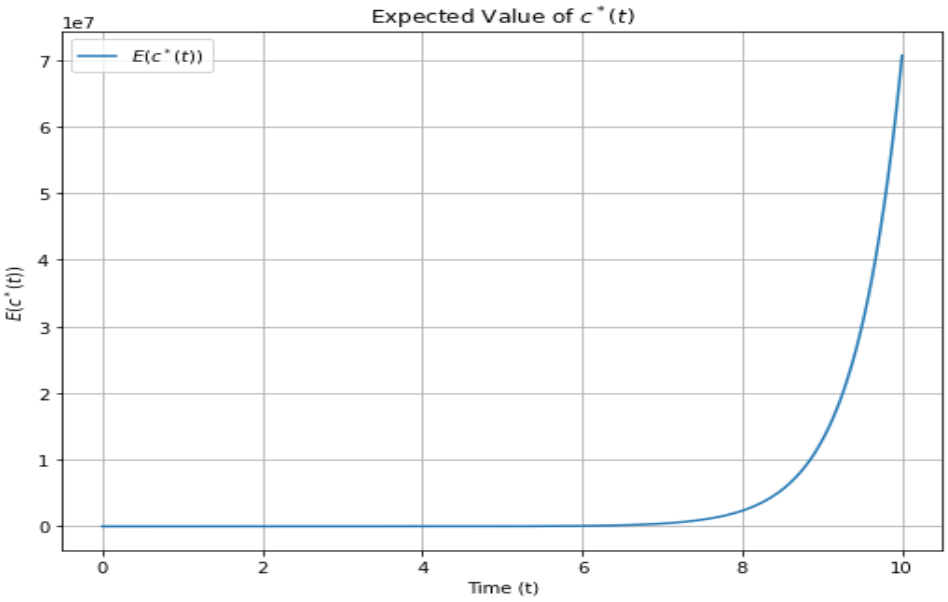

Fig. 7. The concentration of oxygen changes over time

The exponential growth of $E(c_1(t))$ with the given constants demonstrates how oxygen concentration in an ecosystem can increase rapidly over time, driven by initial conditions and influencing parameters. This model underscores the importance of understanding and managing oxygen dynamics to maintain the health and stability of aquatic ecosystems.

4.3 Analysis of enhanced modeling with fractional brownian motion

Fig. (8) shows the effect of the parameter α on the expected values $E(v_1(t))$, $E(u_1(t))$, and $E(c_1(t))$ at t = 0.001. The differences in the curves reflect the different parameters used for each expected value.

Blue Curve $E(v_1(t))$:This curve shows the expected value of $v_1(t)$ as α changes. The constants used are μ_v = 0.1, η_v = 0.7, and σ_{1v} =0.1.

Orange Curve $E(u_1(t))$:This curve shows the expected value of $u_1(t)$ as α changes. The constants used are μ_u =0.2, η_u =0.6 , and σ_{1u} =0.15.

The orange curve is higher than the blue curve, indicating higher expected values due to the different parameters.

Green Curve $E(c_1(t))$: This curve shows the expected value of $c_1(t)$ as α changes. The constants used are μ_c =0.15, η_c = 0.65, and σ_{1c} =0.2.

The green curve is the highest, indicating the highest expected values among the three due to its specific parameters.

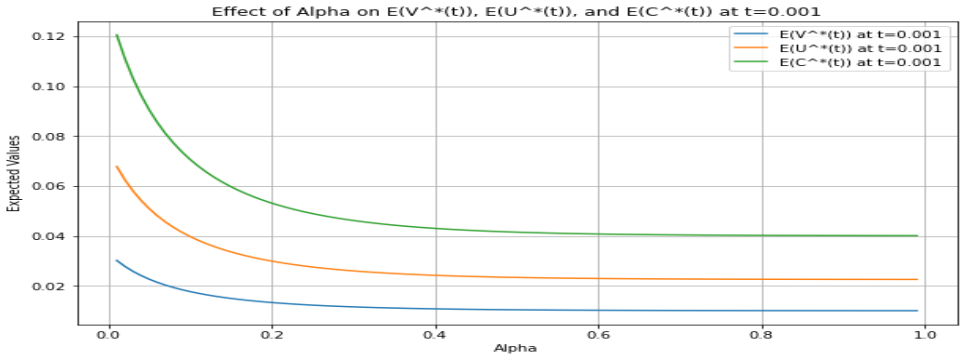

Fig. 8. Comparison between the equations

All three curves exhibit a steep decline initially as α increases from 0. This suggests that all three expected values are highly sensitive to α when α is small. As α approaches 1, the expected values for all three variables level off and change more slowly. The graph clearly shows how different parameters (μ, η, and σ1) affect the expected values $E(v_1(t))$, $E(u_1(t))$, and $E(c_1(t))$ .The relative positions of the curves indicate that with higher values for η and σ1, the expected values tend to be higher.

5 Summary

The study makes a strong connection between its modeling techniques and important facets of climate change, especially when considering oceanic ecosystems.

It is especially admirable that fractional Brownian motion is being used to simulate the intricacies of natural systems.

The study aids in the creation of better-informed and potent countermeasures against the negative effects of climate change.

Related works: Previous research in climate change modeling has extensively utilized various stochastic models to capture the dynamics of rainfall and its broader environmental impacts. Wilks [11] employed a two-state Markov process combined with a mixed exponential distribution to model rainfall occurrence and intensity, finding that this approach provided a better fit compared to the traditional Gamma distribution. Leobacher and Ngare [3] extended this approach by introducing a Markov-Gamma model to capture seasonal variations in monthly precipitation.

Onof [15] explored the challenges associated with Poisson cluster models in rainfall modeling, while Carmona and Diko [16] developed a time-homogeneous jump Markov process to describe rainfall dynamics, modeling rainfall as storms consisting of cells, with changes in intensity represented by a Poisson process. Dzupire, Ngare, and Odongo [5] refined these approaches by introducing a Poisson-Gamma model that addresses both the occurrence and intensity of rainfall, effectively handling zero-inflated data and reducing overdispersion.

Despite the advancements in these traditional models, they often fall short in adequately addressing the issues of overdispersion and zero-inflation in rainfall data, which are crucial for accurate climate modeling. To overcome

these limitations, this research has introduced fractional Poisson and fractional Gamma models, which provide a more robust framework for rainfall modeling and enhance the understanding of climate-related phenomena.

In the context of marine ecosystems, Sekerci and Petrovskii [6] developed a model to examine the impact of global warming on oxygen production by phytoplankton. This study offered foundational insights into how plankton-oxygen systems might respond to ongoing climate change, emphasizing the importance of accurate modeling to predict potential ecological disasters.

Building on these foundational studies, my research donates two key advancements: Incorporating Brownian Motion: To introduce stochastic variability into the plankton-oxygen model, I integrated Brownian motion, enhancing the model's ability to simulate random environmental fluctuations and providing a more realistic representation of natural systems.

Applying Fractional Brownian Motion: Addressing the limitations of previous models, I incorporated fractional Brownian motion to better capture long-term dependencies and nonlinear fluctuations that characterize environmental changes in natural ecosystems.

This research contributes to a deeper understanding of the complex interactions between environmental and biological factors in ecosystems, offering new insights and opening avenues for future research in plankton-oxygen dynamics.

6 Conclusion

This research addresses advanced modeling techniques to tackle the significant challenges posed by climate change, focusing specifically on rainfall modeling and oxygen dynamics in oceanic ecosystems.

Rainfall Modeling: The study introduces the fractional Poisson-Gamma model to enhance the understanding and prediction of rainfall patterns. The model effectively handles datasets with many zero values and reduces overdispersion. It provides a flexible and accurate framework for predicting rainfall, which helps in improving agricultural production, developing weather derivatives, and enhancing hydrological systems.

Oxygen Dynamics in Oceans: The second part of the research focuses on the complex relationship between oceanic ecosystems and climate change, particularly the role of phytoplankton in oxygen production.

Integrated mathematical modeling offers a comprehensive understanding of how changes in oxygen production rates impact the sustainability of oceanic ecosystems.

Fractional Brownian Motion: Incorporating fractional Brownian motion in the modeling provides a powerful tool for capturing randomness and complexity in natural systems. This approach offers a more detailed understanding of the dynamics of phytoplankton and oxygen, aiding in the development of effective strategies for preserving marine ecosystems.

Impact on Climate Change Mitigation Policies: The research highlights the urgent need for advanced and proactive mitigation strategies to address the risks posed by climate change. The advanced modeling techniques presented in this study provide valuable tools for improving predictions and managing the impacts of climate change on vital systems, including rainfall patterns, marine ecosystems, and atmospheric oxygen levels.

In conclusion, this study contributes to the field of climate change research by presenting innovative modeling approaches that enhance our understanding of complex environmental processes. The insights gained from this research are essential for developing informed strategies to mitigate the adverse effects of climate change and ensure the sustainability of natural and human environments. See [17] and [18].

Disclaimer (Artificial Intelligence)

Author(s) hereby declare that NO generative AI technologies such as Large Language Models (ChatGPT, COPILOT, etc) and text-to-image generators have been used during writing or editing of manuscripts.

Acknowledgements

The authors would like to thank the referees and the editors for valuable comments and suggestions on this paper.

Competing Interests

Authors have declared that no competing interests exist.

References

[1] Hussain A. Stochastic modeling of rainfall processes: A Markov chain-mixed exponential model for rainfalls in different climatic conditions. McGill University (Canada); 2008.

[2] Cao M, Li A, Wei JZ. Precipitation modeling and contract valuation. J Altern Invest. 2004;7(2):93-9.

[3] Leobacher G, Ngare P. On modelling and pricing rainfall derivatives with seasonality. Appl Math Finance. 2011;18(1):71-91.

[4] Odening M, Mußhoff O, Xu W. Analysis of rainfall derivatives using daily precipitation models: Opportunities and pitfalls. Agric Finance Rev. 2007;67(1):135-56.

[5] Dzupire NC, Ngare P, Odongo L. A Poisson–gamma model for zero inflated rainfall data. J Prob Stat. 2018;2018(1):1012647.

[6] Sekerci Y, Petrovskii S. Mathematical modelling of plankton–oxygen dynamics under the climate change. Bull Math Biol. 2015;77(12):2325-53.

[7] El-Nadi KE-S. Asymptotic methods and some difference fractional differential equations. Int J Contemp Math Sci. 2006;1(1):3-13.

[8] El-Borai MM. Some probability densities and fundamental solutions of fractional evolution equations. Chaos Solitons Fractals. 2002;14(3):433-40.

[9] Calin O. An informal introduction to stochastic calculus with applications. Singapore: World Scientific; 2015.

[10] Oksendal B. Stochastic differential equations: An introduction with applications. Berlin: Springer Science & Business Media; 2013.

[11] Wilks DS. Multisite generalization of a daily stochastic precipitation generation model. J Hydrol. 1998;210(1):178-91.

[12] El-Borai MM, El-Nadi KE-S. On the construction of a fractional normal distribution and related fractional Brownian motion. Glob Sci J. 2024;12(3).

[13] El-Borai MM, El-Nadi KE-S. On some stochastic nonlinear equations and the fractional Brownian motion. Caspian J Comput Math Eng. 2017;120-23.

[14] El-Borai MM, Moustafa OL, Ahmed HM. Asymptotic stability of some stochastic evolution equations. Appl Math Comput. 2003;144(2):273-86.

[15] Onof C, Chandler RE, Kakou A, Northrop P, Wheater HS, Isham V. Rainfall modelling using Poisson-cluster processes: A review of developments. Stoch Environ Res Risk Assess. 2000;14(6):384-411.

[16] Carmona R, Diko P. Pricing precipitation based derivatives. Int J Theor Appl Finance. 2005;8(7):959-88.

[17] Sattari MT, Bagheri R, Shirini K, Allahverdipour A. Modeling daily and monthly rainfall in Tabriz using ensemble learning models and decision tree regression. Sci J Golestan Univ. 2024;5(18).

[18] Sattari MT, Shirini K, Javidan S. Evaluating the efficiency of dimensionality reduction methods in improving the accuracy of water quality index modeling in Qizil-Uzen River using machine learning algorithms; 1982.

Peer-review history:
The peer review history for this paper can be accessed here (Please copy paste the total link in your browser address bar)
https://www.sdiarticle5.com/review-history/122072